**Keywords:** mpox, global outbreak, effective reproduction number, exponential growth

# Transmission potential of mpox in Mainland China, June-July 2023: estimating reproduction number during the initial phase of the epidemic

**Authors:** Andrei R. Akhmetzhanov, PhD[1,2,*], Pei-Hsuan Wu, MSc[1]

**Affiliations:**

[1] *Institute of Epidemiology and Preventive Medicine, College of Public Health, National Taiwan University, Taipei, Taiwan*

[2] *Global Health Program, College of Public Health, National Taiwan University, Taipei, Taiwan*

**E-mails:** akhmetzhanov@ntu.edu.tw (A.R.A.); s8111127@gmail.com (P.W.)

[*] **Corresponding author:** Andrei R. Akhmetzhanov

College of Public Health, National Taiwan University; No.17 Xuzhou Rd. Zhongzheng District, Taipei 10055, Taiwan; tel: +886-2-3366-8692

# Abstract

**Background**: Despite reporting very few mpox cases early in 2023, Mainland China observed a surge with over 500 cases during the summer. Amid ambiguous prevention strategies and stigma surrounding mpox, the epidemic escalated silently. This study aims to quantify the epidemic scale and assess the transmission dynamics by estimating the effective reproduction number ($R_e$) during its early phase.

**Methods**: Publicly available data sources were aggregated to retrieve daily mpox incidences in Mainland China. The $R_e$ value was estimated employing an exponential growth model. This estimate was compared with $R_e$ values from 16 other national outbreaks in 2022 selected based on a cumulative incidence exceeding 700 symptomatic cases by the end of that year. A meta-analytic approach was adopted to compute the pooled mean of $R_e$ for selected outbreaks.

**Results**: The estimated mean $R_e$ for Mainland China was 1.76 (95% credible interval: 1.51-2.06), suggesting a case doubling time of approximately two weeks. $R_e$ estimates from selected outbreaks of 2022 ranged from 1.17 for Portugal to 2.88 for Columbia. The computed pooled mean stood at 1.66 (1.40-1.92), aligning closely with the $R_e$ for Mainland China.

**Limitations**: The study does not distinguish between indigenous and imported infections, which might impact the $R_e$ estimates. Furthermore, the analysis is limited by reporting delays and underascertainment, especially during the early phase of the epidemic.

**Conclusions**: The initial transmission of mpox in Mainland China appeared largely unchecked, posing potential risks to vulnerable communities. These findings underscore the need for immediate and effective control measures, including targeted vaccination campaigns, to mitigate further spread and impact.

# 1. Introduction

On 9 August 2023, the China Centers for Disease Control (CDC) announced a five-fold increase in mpox cases in Mainland China, with 491 cases in July, a marked escalation from 106 cases in June (1). This surge, though concerning, was largely anticipated by health experts (2, 3). Amid ambiguous prevention strategies and stigmatization of specific groups, especially men who have sex with men (MSM), the mpox epidemic intensified unnoticed.

Mpox is a viral infection mainly transmitted through direct skin-to-skin contact (4). The global mpox outbreak of 2022-2023 was primarily driven by sexual transmission within MSM networks (5). With limited spillover to the broader general population, the 2022 outbreaks predominantly affected high-risk MSM communities (6, 7), making them primary targets for subsequent vaccination campaigns (8, 9).

The global transmission in 2022 was evident, but it was not until 2023 when Western Pacific nations, including Japan, South Korea, and Taiwan, saw significant case counts (10-13). By the end of 2022, many of these countries had minimal or no local mpox transmissions, possibly due to ongoing COVID-19-related travel and social restrictions (14). Given the considerable MSM population in Mainland China, the uncontrollable spread of mpox presents a significant public health concern. An effective mpox vaccine exists, but challenges such as limited accessibility and disease-related stigma have hampered its broad dissemination (2). This underscores the need to understand mpox transmission dynamics in Mainland China and predict the extent of future outbreak evolution.

Epidemics typically follow consistent transmission cycles: introduction, escalation, peaking, and eventual decline (15). The initial stages, often marked by exponential growth, offer important insights into understanding of the disease spread dynamics. The effective reproduction number, $R_e$, is crucial to estimate as it indicates the average number of secondary transmissions per primary case during the period when interventions, behavioral shifts, or acquired immunity have yet to make an impact.

Prior $R_e$ evaluations for the 2022 national mpox outbreaks revealed variability (16-19). Using a sub-exponential growth model, Du and colleagues (16) estimated $R_e$ ranged between 1.02 in Portugal to 1.95 in the United States of America (USA). Conversely, other reports noted higher $R_e$ values, for example, 2.32 and 3.14 were reported for the United Kingdom (UK) (17, 18), comparing to 1.18 estimated by Du et al. (16). While these studies (17, 18) applied variations of a simple susceptible-exposed-infected-recovered (SEIR) model, they also relied on case counts classified by date of reporting. Such an approach can result in estimates biased upward, as it may encompass not just actual transmission dynamics but also the outbreak recognition and discovery of clusters of the infections. Administrative batching in case reporting can further mislead the estimation of $R_e$. Nevertheless, a recent UK mpox study (19) employed a detailed, more complex SEIR model, factoring for potential biases, with $R_e$ changing from 5.16 to 3.02 during the initial stage of the outbreak. Given diverse factors, including cultural differences, differences in outbreak response and challenges with data collection, it is crucial to identify how these estimates align with $R_e$ in Mainland China.

In this study, we analyze the data from the World Health Organization (WHO) and other governmental sources to enhance our understanding of mpox transmission in Mainland China (20-22). By focusing on case counts solely attributed to Mainland China and estimating the $R_e$ during the initial phase of the outbreak, we aim to not only compare it with estimates from 2022, but also project potential case counts to the near future. Our ultimate goal is to inform and potentially optimize the efficiency of ongoing public health interventions and contribute to the global epidemic preparedness.

# 2. Methods

## 2.1. Data collection

This study used three primary data sources. First, daily incidences of confirmed mpox cases in Mainland China, Taiwan, and the Hong Kong Special Administrative Region (SAR) were extracted from the WHO global mpox dashboard (2022-2023) as of 15 August 2023 (20). These incidences were categorized based on the date of symptom onset, followed by the date of diagnosis and the date of reporting. Second, a dataset of daily incidences confirmed in Taiwan, categorized either by the date of symptom onset or by the date of reporting, was retrieved from the National Infectious Disease Statistics System of the Taiwan Centers for Disease Control (CDC) as of 23 August 2023 (21). Third, a linelist of cases confirmed in Hong Kong was compiled using press releases from the Center for Health Protection, the Department of Health of the Government of Hong Kong SAR as of 23 August 2023 (22). In total, the WHO data recorded 859 cases in Mainland China, Taiwan, and Hong Kong. These cases were classified as follows: 615 by date of symptom onset, 225 by date of reporting, and 19 by date of diagnosis.

Independently, the datasets from Taiwan and Hong Kong recorded 292 and 33 cases, respectively, all classified by the date of symptom onset. Notably, one case from Hong Kong lacked a definitive date for symptom onset. The report indicated this case began showing symptoms towards the end of June. For our study, this case was omitted from our analysis as it was reported in August 2023 and was likely not accounted for in the WHO dataset.

To extract cases confirmed solely in Mainland China, the combined daily counts from both Taiwan and Hong Kong datasets were subtracted from the incidences recorded in the WHO dataset. In the process, two different assumptions regarding data decomposition from the WHO dataset were investigated.

First, it was assumed that all counts from Taiwan were reported by date of symptom onset in the WHO dataset. However, upon subtracting these counts from the WHO data, the resulting daily incidence yielded predominantly negative values prior 1 June 2023. Afterwards, only one date of 21 June 2023 appeared with a negative incidence, when the WHO dataset recorded a daily count of two cases, while Taiwan and Hong Kong reported three and zero cases, respectively. This led us to deduce that our initial assumption regarding the integration of Taiwan incidence data into the WHO dataset was likely different.

Thus, we hypothesized that all case counts from Taiwan were incorporated into the WHO dataset by their respective dates of reporting to the WHO. Upon examining the WHO reporting pattern, it became evident that most cases defined by their reporting dates were recorded at equidistant intervals of seven days, specifically on May 2, 9, 16, 23, 30, June 6, 20, 27, and July 4. A single deviation from this pattern was noted: the

inclusion of June 8, but the exclusion of June 13 (**Supplementary Figure 1**). Assuming that the reporting date in Taiwan had a one-day lag from its confirmation date, the case counts from Taiwan aligned almost perfectly with the counts of cases by their reporting dates in the WHO dataset (**Supplementary Figure 2**). While incidences from the Taiwan dataset predominantly fell below the counts of WHO, there was a match in the last five dates: June 8, 20, 27, July 4, and 11. This observation led us to the conclusion that this latter approach to data imputation from Taiwan to the WHO dataset was plausible.

Moreover, the upper bound of the exponential growth phase was set to $t_{up} = 5\ \mathrm{July}\ 2023$, marking the peak of observed daily incidence for symptomatic cases at 21. The exponential growth phase was investigated by considering a 45-day period, placing a lower bound at $t_{lo} = 21\ \mathrm{May}\ 2023$. The robustness of the estimates was explored in the sensitivity analysis by varying the dates for both boundaries, ranged from 16-26 May 2023 for the lower bound and 30 June-10 July 2023 for the upper bound. The duration of the exponential growth phases considered in the sensitivity analysis was thus varied between 15 and 55 days.

## 2.2. Statistical framework

### 2.2.1. Reporting delay distribution

Given that all cases with unidentified symptom onset dates will be back-projected to their estimated date of symptom onset in the subsequent analysis, it becomes crucial to estimate the reporting delay distribution. This distribution measures the time period from the date of symptom onset to either the date of reporting or the date of diagnosis. For

this estimation, we utilized the linelist data from Hong Kong, which composed 33 records, with a cutoff time on $T = 23\ \text{August}\ 2023$.

Each of the reporting delays (time to diagnosis or time to reporting) were fit to the generalized gamma distribution (GGD). The GGD is defined by three parameters: shape $(Q)$, location $(M)$, and scale $(S)$. The choice of GGD was guided by its flexibility and its capability to represent three commonly used distributions: gamma $(\text{when } Q = S)$, Weibull $(\text{when } Q = 1)$, and log-normal $(\text{when } Q = 0)$ (23). The mathematical inference for the GGD was based on the following: if the random variable $x$ follows a GGD, then the transformation $Q\exp(Q^{-2}z)$, where $z = (\log(x) - M)/S$, adheres to a gamma distribution with shape $Q^{-2}$ and scale 1.

In particular, let $O_i$ represent the date of symptom onset, and $D_i$ (where $O_i \leq D_i$) be the date of reporting or diagnosis, extracted from the Hong Kong linelist data with $i = 1, \ldots, 33$. We assume the respective times of symptom onset, $o_i$, and of reporting or diagnosis, $d_i$, to be uniformly distributed within their intervals:

$$\begin{aligned} o_i &\sim \text{Uniform}(O_i, O_i + 1\ \text{day}), \\ d_i &\sim \text{Uniform}(\max(\{o_i, D_i\}), D_i + 1\ \text{day}), \end{aligned} \tag{1}$$

where the symbol "$\sim$" implies "is distributed as". The difference $d_i - o_i$, representing the observed delay, conforms the truncated gamma distribution:

$$y_i \mid y_i \leq Y_i \sim \text{Gamma}(\text{shape} = Q^{-2}, \text{scale} = 1), \tag{2}$$

where: $y_i = Q\exp(Q^{-2}z_i)$, $Y_i = Q\exp(Q^{-2}Z_i)$, and $z_i = (\log(d_i - o_i) - M)/S$, $Z_i = (\log(T - o_i) - M)/S$.

The likelihood writes in the form:

$$L_{\text{rep}}(\theta \mid \{d_i, o_i, T\}) = \prod_i \frac{\gamma(y_i \mid \text{shape} = Q^{-2}, \text{scale} = 1)}{\Gamma(Y_i \mid \text{shape} = Q^{-2}, \text{scale} = 1)}, \tag{3}$$

where $\gamma$ and $\Gamma$ are probability density function (PDF) and cumulative density function (CDF) of the gamma distribution, respectively. The parameters $\theta$ are assumed to have weekly-informative priors: $\log Q\,, M, \log S \sim \text{Normal}(\text{mean} = 0, \text{SD} = 1)$.

### 2.2.2. Reconstructed incidence

Given not all cases were categorized by their date of symptom onset, it was essential to back-project those cases identified solely by their date of diagnosis or reporting to ascertain their presumed date of symptom onset.

Let $n_t$ be the number of cases symptomatic on day $t$, counting from day 1 on $t_{lo}$. Similarly, let $m_t^r$ and $m_t^d$ stand for the cases with unknown symptom onset date but with identified reporting or diagnosis dates, respectively. Any non-zero count $m_t^*$ (where $* := \{r, d\}$) is then back-projected through sampling from a multinomial distribution:

$$\left\{m_{t-s,t}^*; 0 \le s \le t\right\} \sim \text{Multinomial}(\text{size} = m_t^*, \text{probs} = \{f_t^*(s \mid \theta^*)\}). \tag{4}$$

In the above, $f_t^*(x \mid \theta^*)$ describes the discretized reporting delay distribution as:

$$\begin{aligned} f_t^*(0 \mid \theta^*) &= \Gamma(0.5 \mid \theta^*), \\ f_t^*(s \mid \theta^*) &= \Gamma(s + 0.5 \mid \theta^*) - \Gamma(s - 0.5 \mid \theta^*), \qquad s = 1, \dots, t-1, \\ f_t^*(t \mid \theta^*) &= 1 - \sum_{0 \le s \le t-1} f_t^*(s \mid \theta^*) = 1 - \Gamma(t + 0.5 \mid \theta^*). \end{aligned} \tag{5}$$

The final equation in this set indicates the likelihood of a case being reported on day $t$ but manifesting symptoms prior to day 1 (i.e., before $t_{lo}$). To compute the overall incidence, a summation was employed:

$$c_t = n_t + \sum_{x \geq t} m_{t,x}^r + \sum_{x \geq t} m_{t,x}^d, \qquad 1 \leq t \leq T. \tag{6}$$

### 2.2.3. Effective reproduction number ($R_e$) during the initial phase of the epidemic

Earlier, we defined the exponential growth phase using the date range $t_{lo} \leq t \leq t_{up}$. The effective reproduction number, $R_e$, for the initial phase of the epidemic was estimated by analyzing the case counts $c_t$ with the presumption of the exponential growth. The growth rate, $r$, was estimated by incorporating the negative binomial likelihood (24):

$$c_t \sim \mathrm{NegBinom}(\mathrm{mean} = i_0 e^{rt}, \mathrm{overdisp.} = \phi), \tag{7}$$

where $t_{lo} \leq t \leq t_{up}$ and parameters $\{i_0, r, \phi\}$ were supported by weekly-informative priors:

$$\begin{gathered} \log i_0, \log r \sim \mathrm{Normal}(\mathrm{mean} = 0, \mathrm{SD} = 1), \\ \phi \sim \mathrm{Gamma}(\mathrm{shape} = 1, \mathrm{scale} = 1). \end{gathered} \tag{8}$$

$R_e$ was computed based on the formula of Wallinga and Lipsitch (25) that links $R_e$, $r$, and gamma-distributed generation time with the mean $\mu$ and SD $\sigma$:

$$R_e = \exp\left(r\mu - \frac{\sigma^2 \mu^2}{2}\right). \tag{9}$$

For this study, we adopted values $\mu = 12.5$ days and $\sigma = 5.7$ days as estimated in (26).

### 2.2.4. Extrapolation of case counts beyond 5 July 2023

Acknowledging the potential for variations in reported cases due to potential delays or modifications in reporting, we extrapolated the case counts from 5 July 2023 to 1 September under the assumption of sustained exponential growth. The case counts, $\tilde{c}_t$,

which encompass both previously reported and extrapolated, based on symptom onset date, follow the equation:

$$\tilde{c}_t \sim \mathrm{NegBinom}(\mathrm{mean} = i_0 e^{rt}, \mathrm{overdisp.} = \phi), \qquad t > t_{up},$$
$$\tilde{c}_t = c_t, \qquad t \leq t_{up}. \tag{10}$$

Here, "∼" denotes sampling from the negative binomial distribution. The cumulative counts of cases for July and August were derived by aggregating $\tilde{c}_t$ across respective date ranges.

For computing case counts based on the date of reporting, $n_t$, the counts $\tilde{c}_t$ were adjusted considering the reporting delay. For every time $t$, the subsequent sampling was conducted:

$$\{n_{t+s,t}; s > 0\} = \mathrm{Multinomial}(\mathrm{size} = \tilde{c}_t, \mathrm{probs} = \{f_t^*(s \mid \theta^*)\}, \tag{11}$$

where $f_t^*$ refers to (5). Thereafter:

$$n_t = \sum\nolimits_{s \geq 0} n_{t,t-\tau}. \tag{12}$$

Finally, the aggregated count of cases number of cases, $n_t$, for July and August was determined by summation over respective date ranges.

### 2.3. Global trends across outbreaks of 2022

Incidence data on mpox for 2022 was collated from the WHO dashboard (20). Out of this dataset, we selected 16 countries that confirmed over 700 symptomatic cases by the end of the year. The majority of these nations provided daily incidence counts, categorized by date of symptom onset, date of diagnosis, and date of reporting. However, six counties of the WHO Region of Americas (AMRO)—Argentina, Brazil, Chile, Colombia, Mexico, and Peru—presented only aggregated case counts, devoid of

any subtyping. For each country, we identified the exponential growth phase as a 45-day window leading up to the peak of the epidemic, represented by the highest daily case count for 2022. In situations where multiple peaks were recorded, we selected the earliest occurrence. In our sensitivity analysis, we considered alternated windows of 30 and 60 days.

For simplicity, we applied the same reporting delay distribution from Hong Kong data. This seemed reasonable, given its close alignment with globally reported median of 6 days and an inter-quartile spanning the interval of 4-9 days (20), and absence of more detailed global data. Using the methods described earlier, we then estimated the $R_e$ for each of selected countries.

### 2.4. Technical details

We adopted the Bayesian framework to fit each realization of the daily incidence classified by date of symptom onset (6) to respective models (7)-(9) using Markov Chain Monte Carlo (MCMC) sampling techniques. The Bayesian estimation process was carried out using Stan software (27). The inherent structure of the reconstructed incidence posed challenges due to its reliance on sampling backprojected counts from a multinomial distribution (4). Since these counts, represented as integers, are not immediately compatible for the efficient use of Hamilton Monte Carlo (HMC) sampling in Stan, we employed an approach similar to that previously described (28). For each realization of (4), we simulated the MCMC chain using 1,000 iterations for the tuning-in process, and retained only a single posterior for further analysis. To construct the posterior distribution, we used 4,000 different chains, resulting in 4,000 posterior draws. The convergence of the MCMC simulation was inspected visually and was checked

implicitly by fitting the model only for symptomatic cases. In that case, the back-projection was not needed. 1,000 iterations, used for tuning-in, 4 chains composed of 1,000 posterior draws resulted in R-hat statistic below 1.1 (29). The code is made available on http://github.com/aakhmetz/Mpox-in-MainlandChina-2023.

## Results

Analyzing the Hong Kong data, we estimated the mean delay of 3.4 days (95% credible interval [CrI]: 2.7-4.4 days) from symptom onset to case diagnosis, and the mean delay of 6.0 days (95% CrI: 5.1-7.0 days) from symptom onset to case reporting. Upon integrating these delays into the case back-projection (**Figure 1**), the effective reproduction number, $R_e$, was estimated at 1.76 (95% CrI: 1.49-2.06). Correspondingly, the doubling time was found to be 15 days (95% CrI: 11-21 days). Projecting the mpox incidence past 5 July 2023 to cover the whole month of July and August, the mean count of cases categorized by their symptom onset date was at 1,080 cases (95% CrI: 650-1,720) for July and 5,200 (95% CrI: 1,820-12,060) for August. Adjusting these numbers for the reporting delay, the mean number of reported cases stood at 800 cases (95% CrI: 540-1,180) and 3,850 cases (95% CrI: 1,490-8,290) for July and August.

Analysis of national outbreaks from selected countries in 2022 revealed a range in $R_e$ values. Portugal had the lowest at 1.17 (95% CrI: 1.07-1.30), while Columbia had the highest at 2.88 (95% CrI: 2.46-3.34) as illustrated in **Figure 2**. The pooled mean for $R_e$ stood at 1.71 (95% CrI: 1.48-1.95), with a between-countries variance (heterogeneity) of $\tau^2 = 0.19$. However, upon evaluating the data quality provided to the WHO by individual countries, it was evident that nations within the WHO AMRO—with

exceptions of the USA and Canada—provided only aggregated case counts, without subtyping them by date of symptom onset, by date of diagnosis, and by date of reporting. Such reporting likely introduced higher variability and potential bias in the $R_e$ values. By excluding these countries from the analysis, the pooled mean slightly dropped to 1.66 (95% CrI: 1.40-1.92), and the between-country variance reduced to $\tau^2 = 0.15$. Notably, the $R_e$, value for Mainland China remained consistent with the pooled average, regardless of whether AMRO countries were included or excluded from the analysis.

The sensitivity analysis confirmed the robustness of our findings but highlighted some variability. Considering only for cases with a known symptom onset date, the $R_e$ for Mainland China remained consistent at 1.75 (95% CrI: 1.48-2.05), suggesting most cases classified by the date of reporting were predominantly linked to Taiwan. Varying the time window for identified exponential growth phase—where the lower bound, $t_{lo}$, varied between 16 May 2023 and 26 June 2023, and the upper bound, $t_{up}$, varied between 30 June 2023 and 10 July 2023—the median posterior of $R_e$ ranged 1.58-1.72 (95% CrI 1.38-2.05) (**Supplementary Figure 3**). The posterior predictions for reported cases ranged 650-840 (95% CrI: 480-1,400) for July and 2,150-3,540 (95% CrI: 1,110-9,690) for August (**Supplementary Figure 4, Supplementary Figure 5**). For the selected outbreaks of 2022, adjusting the length of the exponential growth phase to either 30 or 60 days did not critically alter the prior estimates (**Supplementary Figure 6**). Importantly, when focusing solely on cases with known symptom onsets, $R_e$ estimated remained unchanged, indicating the minimal effect of case records with unknown symptom onset on the $R_e$ for the selected countries.

# Discussion

In our analysis, we estimated the effective reproduction number, $R_e$, of the mpox epidemic in Mainland China to fall within the range of 1.6-1.8. This value suggests a doubling time of approximately two weeks. It is important to note that our estimate is based on early phase of the epidemic, where there is evident exponential growth of cases, and it is likely that control measures have not yet been implemented. Given the relatively low incidence and no deaths reported during that period, significant behavioral changes in the populations at risk were probably not yet in effect. This implies that, at this stage, the transmission of mpox occurred largely unhindered within affected communities.

The $R_e$ value estimated in our study closely aligns with those derived from selected national outbreaks of 2022, implying a probably universal character of the outbreaks. However, an accurate estimation of the infections remains challenging due to probable underreporting of mpox cases. Several factors might contribute to this underascertainment. One reason could be societal stigmatization associated with the disease, where individuals might be reluctant to disclose their infection for fear of facing societal prejudice or discrimination. Another possibility is infections resulting from intimate encounters outside a committed relationship, leading individuals to withhold their status due to concerns over potential repercussions in their personal lives. As a consequence, most cases in the dataset might be those that were either severe in nature or detected through active surveillance measures, such as those implemented at entry points into Mainland China.

Our study has several limitations. First, we did not differentiate between indigenous and imported infections in our dataset, a factor that could influence the $R_e$ estimation. Yet, by focusing only on the exponential phase, where case growth is most evident, we believe that the influence of imported cases on our estimates was likely minimal. Second, the actual way how cases from Taiwan were imputed in the WHO dataset might differ from ours or could have been modified by the WHO over time. For example, the observed pattern of data imputations by given dates of reporting aggregated every seven days was not feasible anymore at the end of July and August. Third, the reporting delay distribution was estimated using a Hong-Kong linelist data. This might differ from data in Mainland China, given differences in healthcare systems, case ascertainment, and case investigation protocols. Fourth, when comparing $R_e$ across different countries, we still much consider the results with caution. The proactive control measures adopted by some nations versus the more passive strategies employed by others can introduce variances. For instance, the outbreak in Portugal evolved at slower pace due to proactive position of the government. The case counts were almost steady over two to three months before witnessing a decline. While the $R_e$ in our study and that of Du et al. (16) was close to one, a granular look at the case counts, combined with a time-varying $R_e$, revealed a brief peak of $R_e$ at 2.7 on 10 May 2022, which then gradually declined towards one, dropping below this threshold by the end of June 2022 (30). Our mathematical framework successfully captured this average trend across Portugal and other countries, with a pooled mean of 1.66 summarized our overall knowledge. Lastly, the WHO dataset retrieved on 15 August 2023 contained incomplete case counts with some cases yet to be reported. Indeed, at the time of

writing the results of this study, another snapshot of 12 September 2023 became available. The $R_e$ estimate was only slightly changed to 1.63 (95% CrI: 1.43-1.86), but the case counts for May and June were still updated revealing possible long reporting delays (*cf.* **Supplementary Figure 7** and **Supplementary Figure 1A**).

While mpox might exhibit a lower mortality rate compared to diseases like smallpox, its morbidity can be notably high with health complications, such as pneumonia, confusion, or eye infections (31), and disproportionally affecting people living with HIV (32). The transmission of mpox throughout Mainland China in the summer of 2023 was largely unconstrained, given that regulatory guidelines were first published only at the end of July. This timeline put vulnerable populations at heightened risk of infections and subsequent complications. Nevertheless, the potential impact of efficient vaccination campaigns and information programs aimed at raising awareness of the disease cannot be overlooked; such interventions could significantly reduce case numbers and prevent a larger outbreak in the future. In contrast to Mainland China, Taiwan managed to stabilize its mpox situation in 2023, maintaining $R_e$ around one. Drawing from their previous experience—specifically, their management of the hepatitis A virus (HAV) outbreak among MSM in 2015-2017 (33)—the Taiwan government promptly initiated a vaccination campaign, targeted high-risk groups, and was bolstered by awareness campaign. This strategy not only ensured low vaccine hesitancy, but also prevented an escalating outbreak. Mainland China could adopt a similar approach, focusing the vaccination campaigns on high-risk social groups coupled with dissemination of accurate health messages. Avoidance of stigmatization of the disease

could further contribute to higher vaccination rates, an oversight seen during the early stages of the outbreak (2, 3).

## Financial support

This study was supported by the National Science and Technology Council, Taiwan (NSTC #111-2314-B-002-289).

## Conflict of interest

The authors declare that there are no known competing financial or personal relationships that could have appeared to influence the work reported in this paper.

## Ethical standards

This study was based on publicly available data and did not require ethical approval.

## Data availability statement

All data used for this study can be found at: http://github.com/aakhmetz/Mpox-in-MainlandChina-2023/data

371 # References


372 1. China Centers for Disease Control. Mpox epidemic monitoring situation in July
373 2023 [in Chinese]. 2023 [cited 12 September 2023]; Available from:
374 https://www.chinacdc.cn/jkzt/crb/qt/szkb_13037/gwjszl_13092/202308/t20230809_2685
375 02.html
376 2. Murphy F. Mpox: China's health authorities fight surge in cases of unknown
377 origin. BMJ. 2023;382:p1939. https://doi.org/10.1136/bmj.p1939
378 3. Yang Z. China is suddenly dealing with another public health crisis: mpox. MIT
379 Technology Review. 2023 [cited 1 August 2023]; Available from:
380 https://www.technologyreview.com/2023/08/01/1077047/china-public-health-crisis-
381 mpox-outbreak/
382 4. The United States Centers for Disease Control and Prevention. Mpox: how it
383 spreads. 2023 [cited 12 September 2023]; Available from:
384 https://www.cdc.gov/poxvirus/mpox/if-sick/transmission.html
385 5. Thornhill JP, Barkati S, Walmsley S, Rockstroh J, Antinori A, Harrison LB, et al.
386 Monkeypox Virus Infection in Humans across 16 Countries — April–June 2022. New
387 England Journal of Medicine. 2022;387(8):679-91.
388 https://doi.org/10.1056/NEJMoa2207323
389 6. Endo A, Murayama H, Abbott S, Ratnayake R, Pearson CAB, Edmunds WJ, et
390 al. Heavy-tailed sexual contact networks and monkeypox epidemiology in the global
391 outbreak, 2022. Science. 2022 Oct 7;378(6615):90-4.
392 https://doi.org/10.1126/science.add4507
393 7. Murayama H, Pearson CAB, Abbott S, Miura F, Jung S-m, Fearon E, et al.
394 Accumulation of Immunity in Heavy-Tailed Sexual Contact Networks Shapes Mpox
395 Outbreak Sizes. The Journal of Infectious Diseases. 2023.
396 https://doi.org/10.1093/infdis/jiad254
397 8. Chitwood MH, Kwon J, Savinkina A, Walker J, Bilinski A, Gonsalves G.
398 Estimated Testing, Tracing, and Vaccination Targets for Containment of the US Mpox
399 Outbreak. JAMA Network Open. 2023;6(1):e2250984-e.
400 https://doi.org/10.1001/jamanetworkopen.2022.50984

9. Vairo F, Leone S, Mazzotta V, Piselli P, De Carli G, Lanini S, et al. The possible effect of sociobehavioral factors and public health actions on the mpox epidemic slowdown. International Journal of Infectious Diseases. 2023 2023/05/01/;130:83-5. https://doi.org/10.1016/j.ijid.2023.03.005

10. Nishiura H, Hayashi K, Anzai A, Kobayashi T, Miyama T, Ueda M, et al. Upcoming major epidemic of mpox in Japan, 2022-23. ResearchGate Preprint. 2023. https://doi.org/10.13140/RG.2.2.34892.08327

11. Kim T, Park E, Eun JS, Lee EY, Mun JW, Choi Y, et al. Detecting mpox infection in the early epidemic: an epidemiologic investigation of the third and fourth cases in Korea. Epidemiol Health. 2023;45:e2023040. https://doi.org/10.4178/epih.e2023040

12. Chan PC, Lee CC. Response to Mpox transmission - Taiwan, Jan 1 -May 11, 2023. J Formos Med Assoc. 2023 Sep;122(9):819-21. https://doi.org/10.1016/j.jfma.2023.06.019

13. Endo A, Jung S-m, Miura F. Mpox emergence in Japan: ongoing risk of establishment in Asia. The Lancet. 2023;401(10392):1923-4. https://doi.org/10.1016/S0140-6736(23)00766-3

14. Akhmetzhanov AR, Ponce L, Thompson RN. Emergence potential of monkeypox in the Western Pacific Region, July 2022. International Journal of Infectious Diseases. 2022 2022/09/01/;122:829-31. https://doi.org/10.1016/j.ijid.2022.07.044

15. Linton NM, Lovell-Read FA, Southall E, Lee H, Akhmetzhanov AR, Thompson RN, Nishiura H. When Do Epidemics End? Scientific Insights from Mathematical Modelling Studies. Centaurus. 2022;64(1):31-60. https://doi.org/10.1484/j.Cnt.5.130125

16. Du Z, Shao Z, Bai Y, Wang L, Herrera-Diestra JL, Fox SJ, et al. Reproduction number of monkeypox in the early stage of the 2022 multi-country outbreak. Journal of Travel Medicine. 2022;29(8). https://doi.org/10.1093/jtm/taac099

17. Liu T, Yang S, Luo B, Fan X, Zhuang Y, Gao GF, et al. Anticipating the transmissibility of the 2022 mpox outbreak. Journal of Medical Virology. 2023;95(3):e28683. https://doi.org/https://doi.org/10.1002/jmv.28683

18. Yang S, Guo X, Zhao Z, Abudunaibi B, Zhao Y, Rui J, et al. Possibility of mpox viral transmission and control from high-risk to the general population: a modeling study.

BMC Infectious Diseases. 2023 2023/02/24;23(1):119. https://doi.org/10.1186/s12879-023-08083-5

19. Brand SPC, Cavallaro M, Cumming F, Turner C, Florence I, Blomquist P, et al. The role of vaccination and public awareness in forecasts of Mpox incidence in the United Kingdom. Nat Commun. 2023 Jul 11;14(1):4100. https://doi.org/10.1038/s41467-023-38816-8

20. World Health Organization. 2022-23 Mpox (Monkeypox) Outbreak: Global Trends. 2023 [cited 23 August 2023]; Available from: https://worldhealthorg.shinyapps.io/mpx_global/

21. Taiwan Centers for Disease Control. Taiwan National Infectious Disease Statistics System. 2023 [cited 23 August 2023]; Available from: https://nidss.cdc.gov.tw/en/nndss/disease?id=MPXV

22. The Government of the Hong Kong Special Administrative Region. Center for Health Protection, Department of Health. Mpox (also known as monkeypox). 2023 [cited 23 August 2023]; Available from: https://www.chp.gov.hk/en/miniweb/press_release/100155.html

23. Hoffmann T, Alsing J. Faecal shedding models for SARS-CoV-2 RNA among hospitalised patients and implications for wastewater-based epidemiology. Journal of the Royal Statistical Society Series C: Applied Statistics. 2023;72(2):330-45. https://doi.org/10.1093/jrsssc/qlad011

24. Ma J. Estimating epidemic exponential growth rate and basic reproduction number. Infect Dis Model. 2020;5:129-41. https://doi.org/10.1016/j.idm.2019.12.009

25. Wallinga J, Lipsitch M. How generation intervals shape the relationship between growth rates and reproductive numbers. Proc Biol Sci. 2007 Feb 22;274(1609):599-604. https://doi.org/10.1098/rspb.2006.3754

26. Guzzetta G, Mammone A, Ferraro F, Caraglia A, Rapiti A, Marziano V, et al. Early Estimates of Monkeypox Incubation Period, Generation Time, and Reproduction Number, Italy, May-June 2022. Emerging infectious diseases. 2022;28(10):2078-81. https://doi.org/10.3201/eid2810.221126

27. Stan Development Team. Stan modeling language users guide and reference manual, 2.33.0. 2023 [cited 23 August 2023]; Available from: https://mc-stan.org

28. Weber S, Gelman A, Lee D, Betancourt M, Vehtari A, Racine-Poon A. Bayesian aggregation of average data: An application in drug development. The Annals of Applied Statistics. 2018;12(3):1583-604, 22. https://doi.org/10.1214/17-AOAS1122

29. Vehtari A, Gelman A, Simpson D, Carpenter B, Bürkner P-C. Rank-Normalization, Folding, and Localization: An Improved $\widehat{R}$ for Assessing Convergence of MCMC (with Discussion). Bayesian Analysis. 2021;16(2):667-718, 52.

30. Borges V, Duque MP, Martins JV, Vasconcelos P, Ferreira R, Sobral D, et al. Viral genetic clustering and transmission dynamics of the 2022 mpox outbreak in Portugal. Nature Medicine. 2023 2023/09/11. https://doi.org/10.1038/s41591-023-02542-x

31. Patel VM, Patel SV. Epidemiological Review on Monkeypox. Cureus. 2023 Feb;15(2):e34653. https://doi.org/10.7759/cureus.34653

32. Mitjà O, Alemany A, Marks M, Lezama Mora JI, Rodríguez-Aldama JC, Torres Silva MS, et al. Mpox in people with advanced HIV infection: a global case series. The Lancet. 2023;401(10380):939-49. https://doi.org/10.1016/S0140-6736(23)00273-8

33. Lin K-Y, Sun H-Y, Chen Y-H, Lo Y-C, Hsieh S-M, Sheng W-H, et al. Effect of a Hepatitis A Vaccination Campaign During a Hepatitis A Outbreak in Taiwan, 2015–2017: A Modeling Study. Clinical Infectious Diseases. 2019;70(8):1742-9. https://doi.org/10.1093/cid/ciz471

# Figures

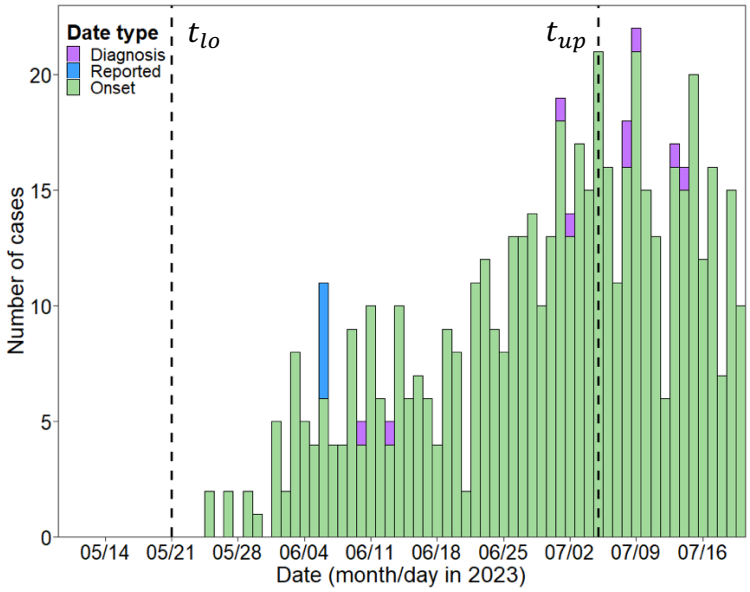


**Figure 1: The estimation of the case back-projection for Mainland China, integrating reporting delays.** The exponential growth phase with dashed lines, representing the lower bound, $t_{lo}$, on 21 May 2023, and the upper bound, $t_{up}$, on 5 July 2023.

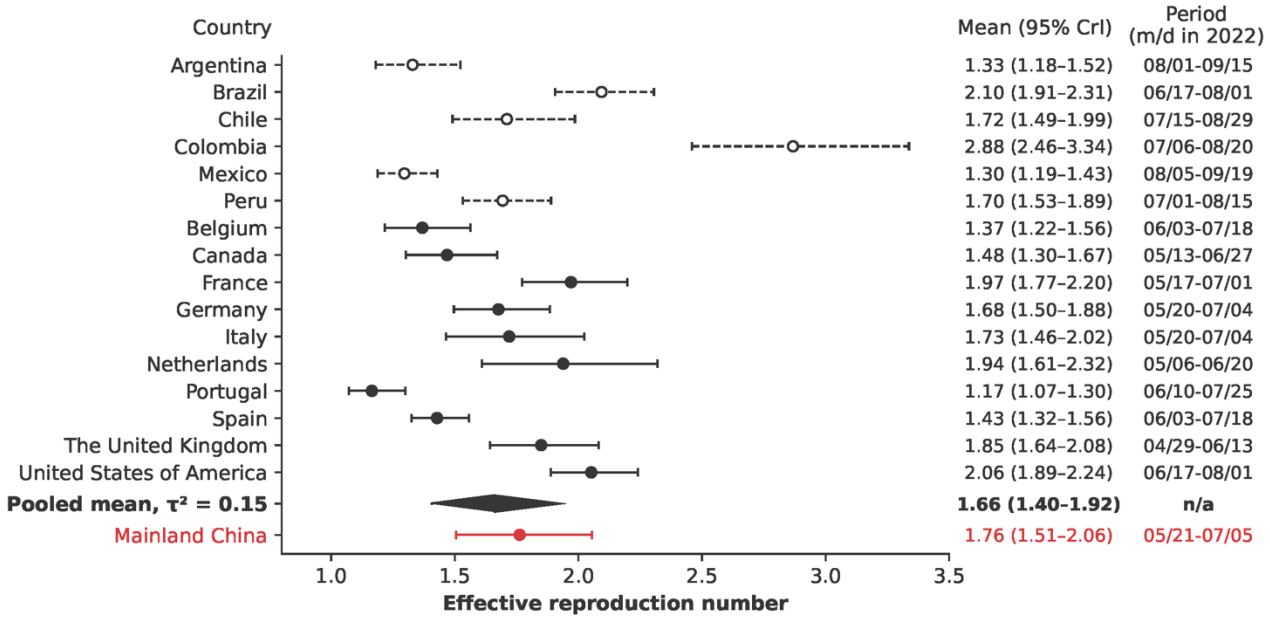


**Figure 2: Estimated effective reproduction number, $R_e$, for Mainland China (red) comparing to selected national outbreaks of 2022 (black) and their pooled mean (black diamond).** The $R_e$ values are shown in the first column on the right, while a time period of 45 days is indicated in the last column. Countries that have not reported case counts, subtyped by date of symptom onset, diagnosis date, and reporting dates, were excluded from calculation of the pooled mean and are shown in dashed black.

# Supplementary Materials

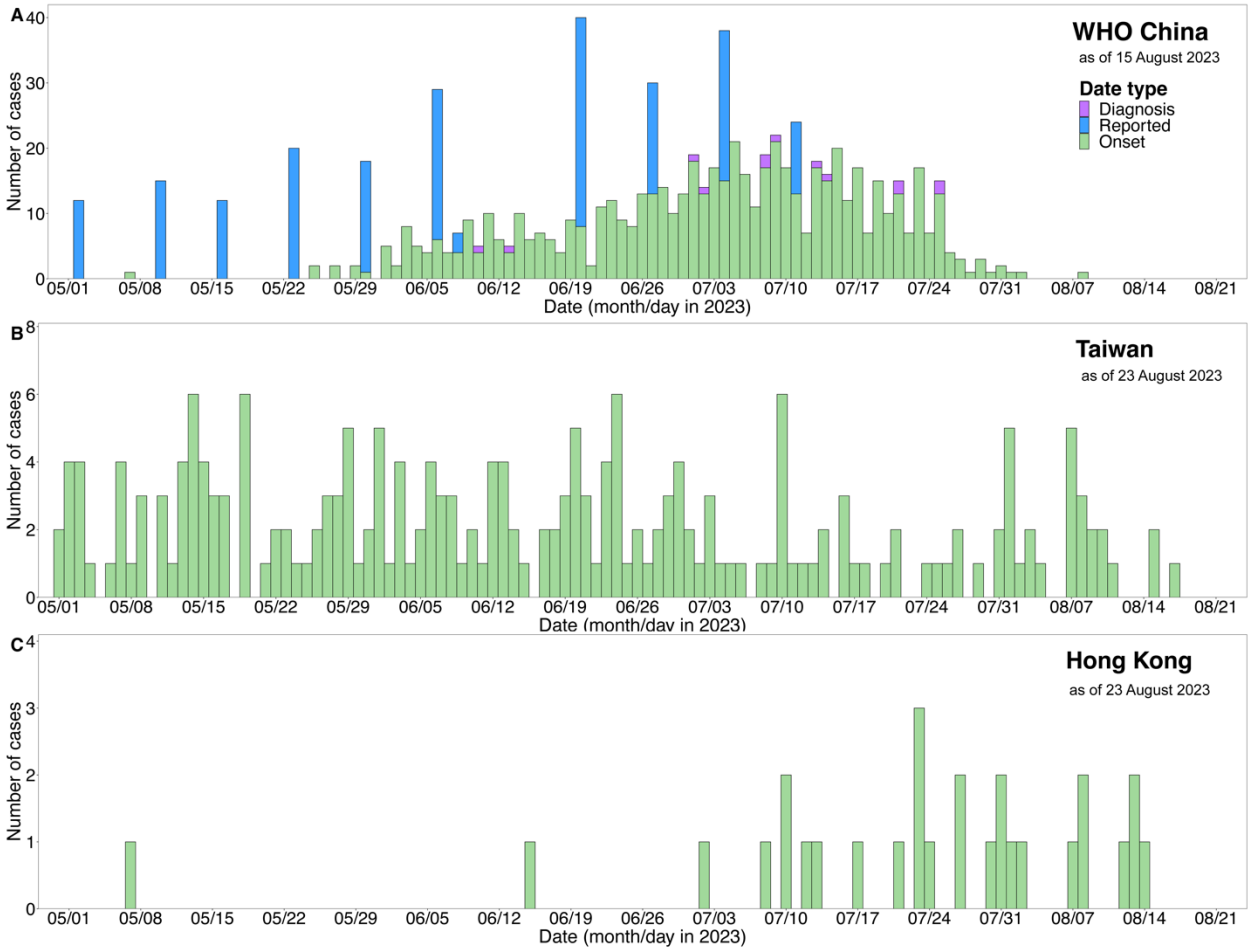


**Supplementary Figure 1: Daily incidences reported by the World Health Organization (A), Taiwan Centers for Disease Control (B) and the Government of the Hong Kong Special Administrative Region (C).** The snapshot dates are indicated in the legends. Each case count is subtyped by the date of symptom onset, the date of diagnosis, and the date of reporting.

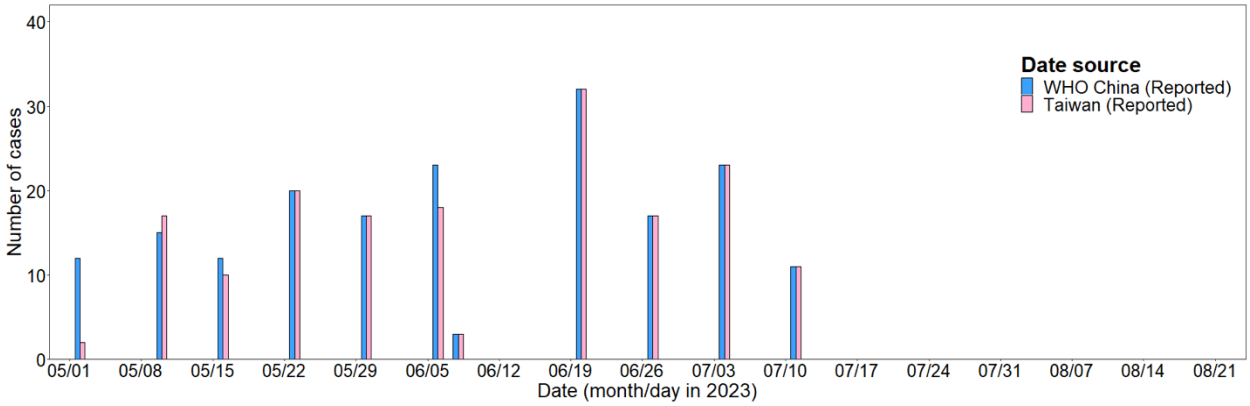


**Supplementary Figure 2: The concordance in case counts between the World Health Organization (WHO) dataset (blue; as of 15 August 2023) and Taiwan Centers for Disease Control (pink; as of 23 August 2023) that were aggregated by date of reporting.** The dates of reporting for Taiwan were aggregated to the dates of reporting from the WHO dataset and Taiwan cases beyond the latest 11 July 2023 were omitted.

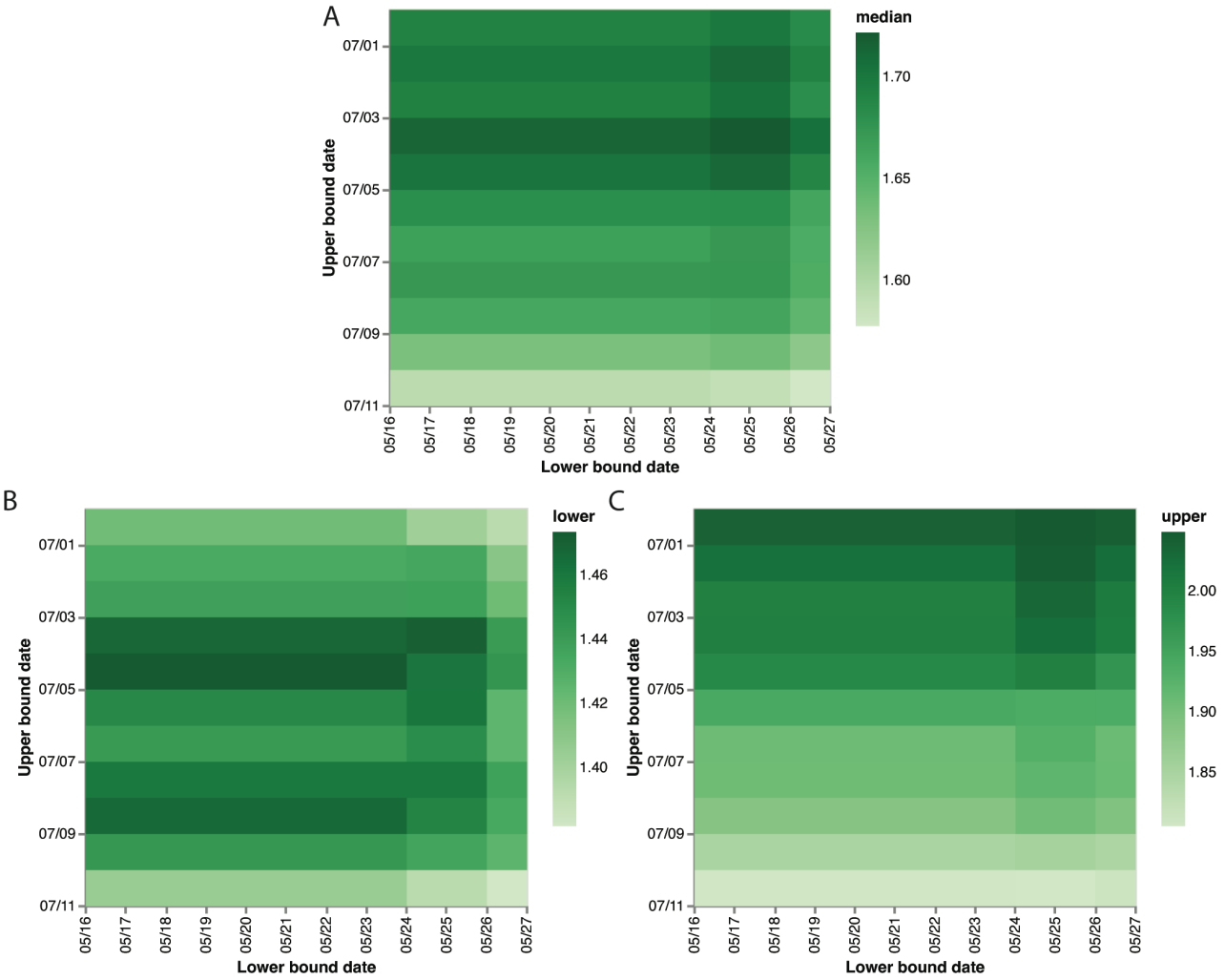


**Supplementary Figure 3: Effective reproduction number, $R_e$, during the initial phase of the epidemic in Mainland China depending on the time window identifying the exponential phase.** (A) shows the posterior median of $R_e$, (B) and (C) show the lower (2.5$^{th}$ percentile) and upper (97.5$^{th}$ percentile) bound of the 95% credible interval, respectively. Horizontal axis indicates the lower bound, while the vertical axis indicates the upper bound which were used for the exponential phase window. The date is indicated as month/day in 2023.

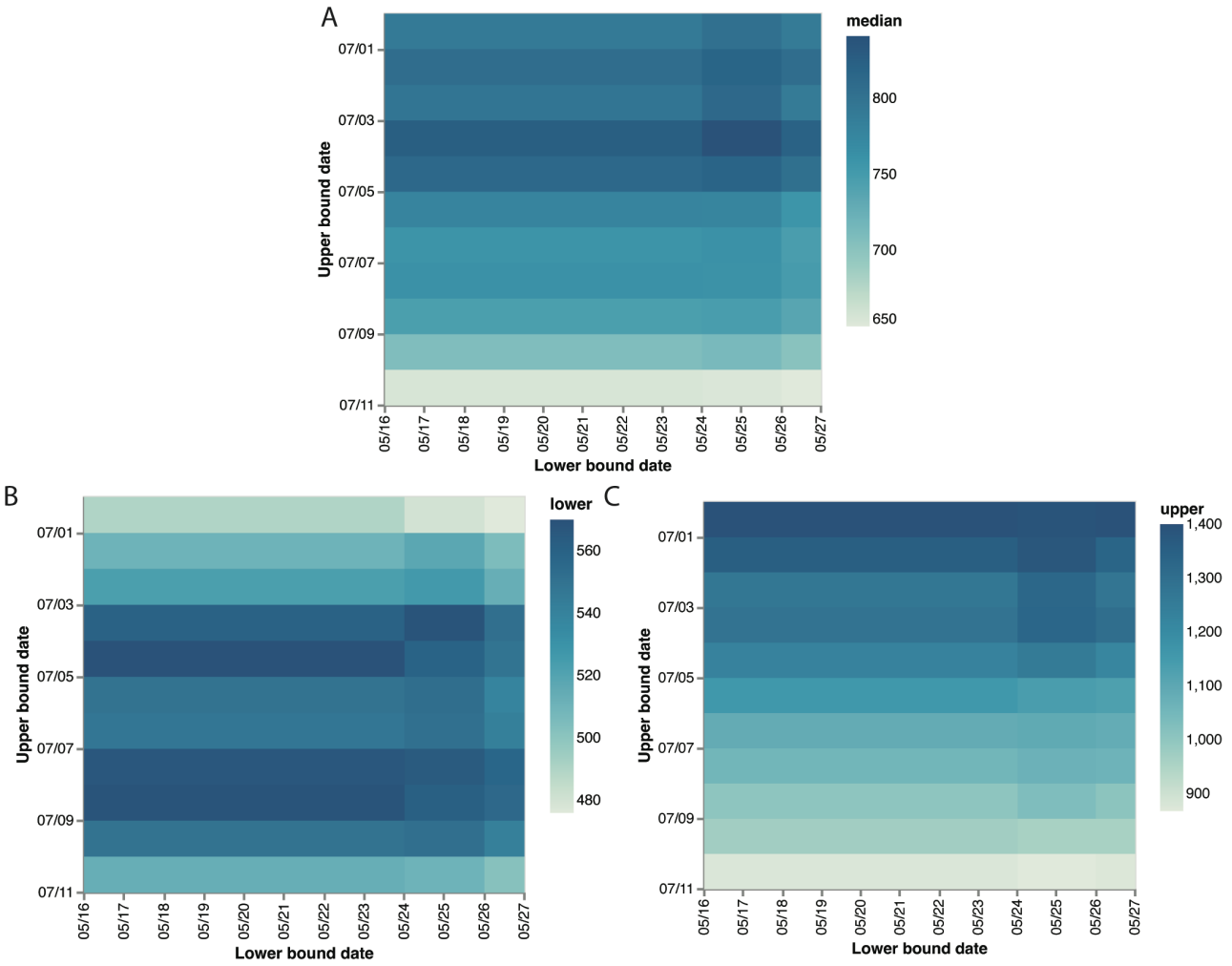


**Supplementary Figure 4: Predicted number of reported cases in July depending on the time window identifying the exponential phase.** (A) shows the posterior median of number of cases, (B) and (C) show the lower (2.5$^{th}$ percentile) and upper (97.5$^{th}$ percentile) bound of the 95% credible interval, respectively. Horizontal axis indicates the lower bound date, while the vertical axis indicates the upper bound which were used for the exponential phase window. The date is indicated as month/day in 2023.

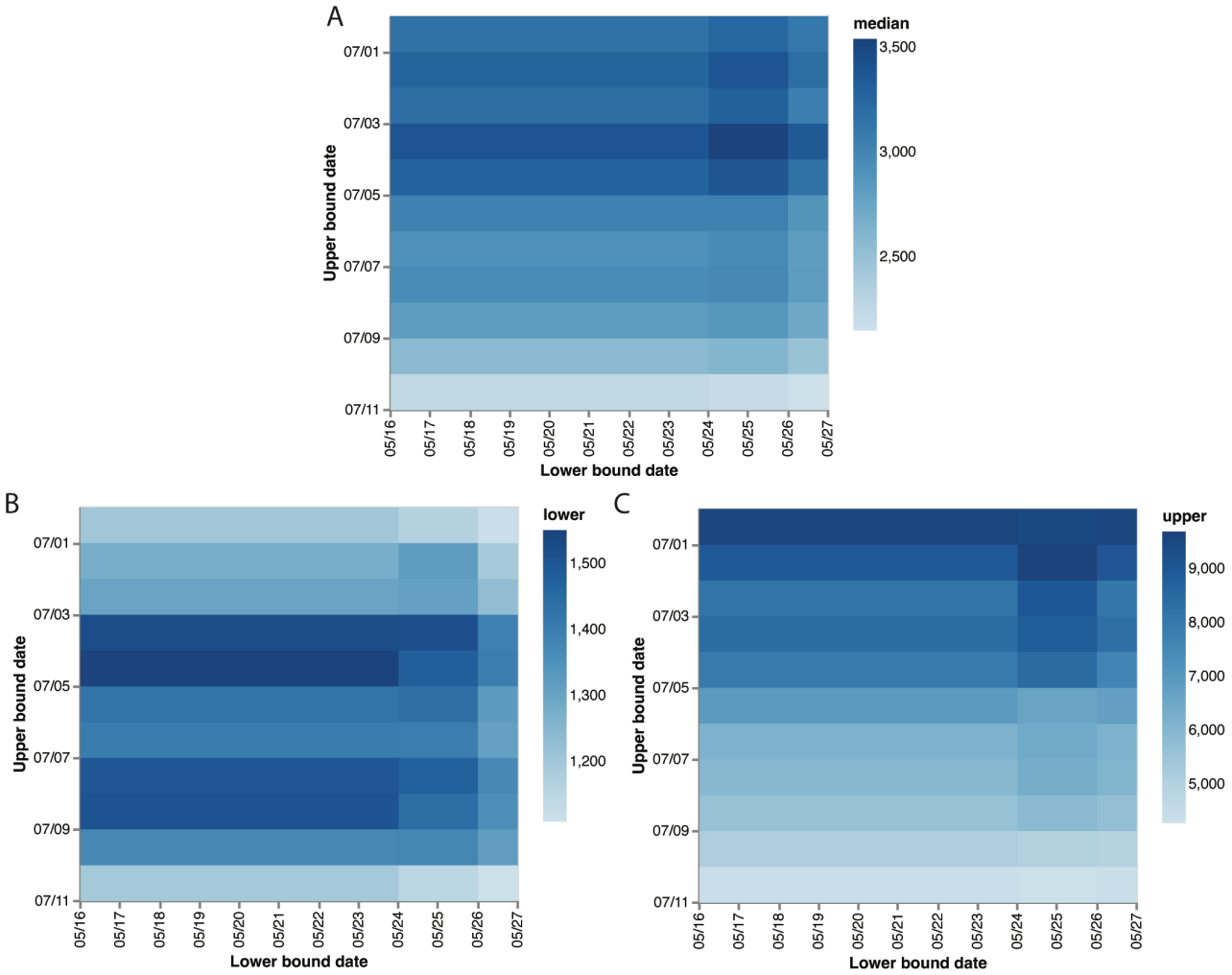


**Supplementary Figure 5: Predicted number of reported cases in August depending on the time window identifying the exponential phase.** (A) shows the posterior median of number of cases, (B) and (C) show the lower (2.5$^{th}$ percentile) and upper (97.5$^{th}$ percentile) bound of the 95% credible interval, respectively. Horizontal axis indicates the lower bound date, while the vertical axis indicates the upper bound which were used for the exponential phase window. The date is indicated as month/day in 2023.

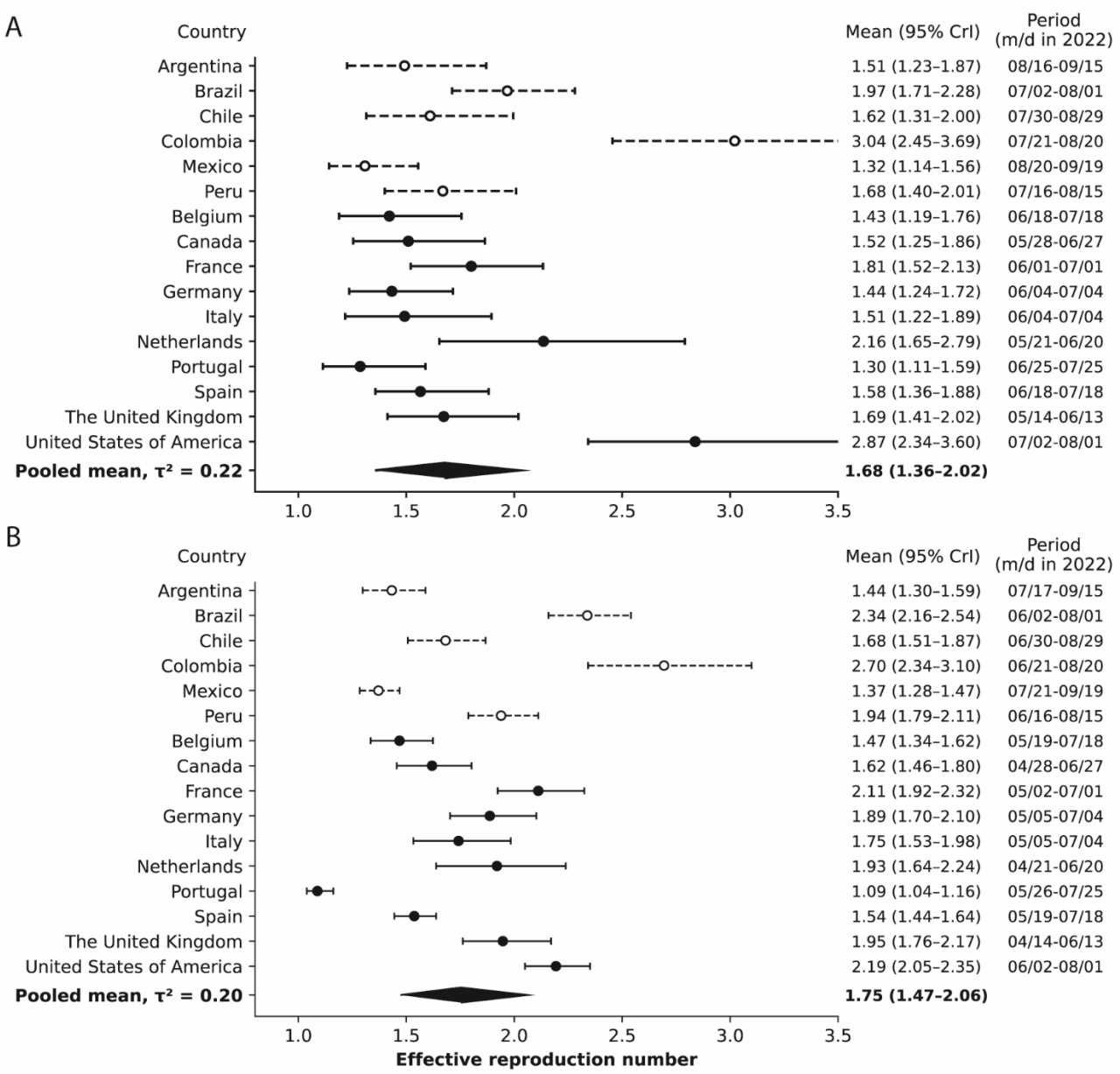


**Supplementary Figure 6: Effective reproduction number across selected national mpox outbreaks of 2022.** The $R_e$ values are shown in the first column on the right, while a time period of 30 days (A) or 60 days (B) is indicated in the last column. Countries that have not reported case counts, subtyped by date of symptom onset, diagnosis date, and reporting dates, were excluded from calculation of the pooled mean and are shown in dashed black.

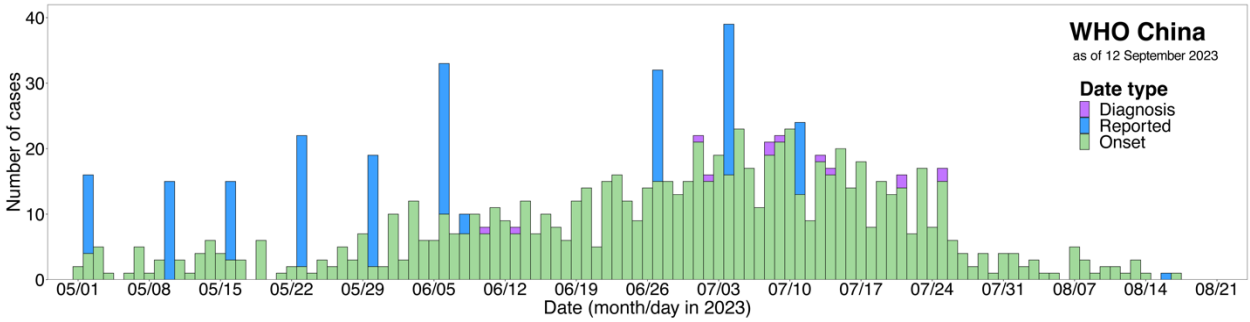


**Supplementary Figure 7: Daily incidences reported by the World Health Organization (WHO) with the snapshot date of 12 September 2023.** Each case count is subtyped by the date of symptom onset, the date of diagnosis, and the date of reporting.